Exp Brain Res (1997) 117:30–42

RESEARCH ARTICLE

D.J. Newman · D.K. Jackson · J.J. Bloomberg

Altered astronaut lower limb and mass center kinematics in downward jumping following space flight

Received: 13 February 1996 / Accepted: 14 April 1997

Abstract Astronauts exposed to the microgravity conditions encountered during space flight exhibit postural and gait instabilities upon return to earth that could impair critical postflight performance. The aim of the present study was to determine the effects of microgravity exposure on astronauts' performance of two-footed jump landings. Nine astronauts from several Space Shuttle missions were tested both preflight and postflight with a series of voluntary, two-footed downward hops from a 30-cm-high step. A video-based, three-dimensional motion-analysis system permitted calculation of body segment positions and joint angular displacements. Phase-plane plots of knee, hip, and ankle angular velocities compared with the corresponding joint angles were used to describe the lower limb kinematics during jump landings. The position of the whole-body center of mass (COM) was also estimated in the sagittal plane using an eight-segment body model. Four of nine subjects exhibited expanded phase-plane portraits postflight, with significant increases in peak joint flexion angles and flexion rates following space flight. In contrast, two subjects showed significant contractions of their phase-plane portraits postflight and three subjects showed insignificant overall changes after space flight. Analysis of the vertical COM motion generally supported the joint angle results. Subjects with expanded joint angle phase-plane portraits postflight exhibited larger downward deviations of the COM and longer times from impact to peak deflection, as well as lower upward recovery velocities. Subjects with postflight joint angle phase-plane contraction demonstrated opposite effects in the COM motion. The joint kinematics results indicated the existence of two contrasting response modes due to microgravity exposure. Most subjects exhibited "compliant" impact absorption postflight, consistent with decreased limb stiffness and damping, and a reduction in the bandwidth of the postural control system. Fewer subjects showed "stiff" behavior after space flight, where contractions in the phase-plane portraits pointed to an increase in control bandwidth. The changes appeared to result from adaptive modifications in the control of lower limb impedance. A simple 2nd-order model of the vertical COM motion indicated that changes in the effective vertical stiffness of the legs can predict key features of the postflight performance. *Compliant* responses may reflect inflight adaptation due to altered demands on the postural control system in microgravity, while *stiff* behavior may result from overcompensation postflight for the presumed reduction in limb stiffness inflight.

Key words Kinematics · Impedance · Jumping · Posture control · Astronaut performance · Human

Introduction

A variety of studies of astronaut performance following space flight indicate that exposure to microgravity can cause profound changes in human balance, posture control, and locomotion. Kenyon and Young (1986) found decrements in standing ability with the eyes closed for several days following space flight; subjects were only able to maintain upright posture if they stayed within a very narrow cone of static stability near the vertical (Young et al. 1986). In posture platform tests, astronauts demonstrated abnormal postural sway oscillations and drift immediately postflight when the support was sway-referenced to eliminate ankle proprioception cues (Paloski et al. 1993). Watt et al. (1986) tested astronauts subjected to sudden "drops" and reported that all subjects were unsteady postflight and that one subject fell over backward consistently.

Anecdotal descriptions of astronaut locomotion postflight reveal abnormalities in walking, including adapting

D.J. Newman (✉) · D.K. Jackson
Department of Aeronautics and Astronautics, Massachusetts Institute of Technology, 77 Massachusetts Avenue, Rm. 33-119, Cambridge, MA 02139, USA
Tel.: +1-617-258-8799, Fax: +1-617-253-4196, e-mail: dnewman@mit.edu

J.J. Bloomberg
Life Sciences Research Laboratories, NASA Johnson Space Center, USA

a wide stance during gait and difficulty in rounding corners (Homick and Reschke 1977). Chekirda et al. (1971) also reported a "stamping" gait, shift of the body toward the support leg, and deviations from straight paths while walking on the 1st day following space flight. Recently, Bloomberg et al. (1997) observed alterations in head-trunk coordination during locomotion that may contribute to postflight postural and locomotion disturbances.

Such performance decrements may result from various changes in the sensorimotor complex due to microgravity exposure. Parker et al. (1985) found direct evidence for reinterpretation of graviceptor inputs during space flight. Young et al. (1986) also provided evidence for sensory compensation during space flight, resulting in interpretation of utricular otolith signals as linear acceleration rather than head tilt, as well as increased dependence on visual cues for perception of orientation. The otolith-spinal reflex, which helps prepare the leg musculature for impact in response to sudden falls, is dramatically reduced during space flight (Watt et al. 1986). However, postflight results were not significantly different from preflight responses, indicating a rapid course of readaptation upon return to earth. Other work indicates that space flight may affect proprioception of limb position: Watt et al. (1985) found a considerable decline in arm-pointing accuracy while blindfolded during and immediately following space flight. Furthermore, the subject who fell consistently in the drop test reported that his legs were always further forward than he expected them to be.

Other possible explanations for postflight postural instability include atrophy of the antigravity muscles (Martin et al. 1988), inflight changes in tonic leg muscle activation patterns, or microgravity-induced alterations in stretch reflexes (Gurfinkel 1994; Layne et al. 1995). Gurfinkel also reported reorganization of higher-level anticipatory postural responses to rapid movements during space flight. Altered patterns of leg muscle coactivation may result in changes in the modulation of limb impedance that controls the dynamic interaction of the limb with the environment. McDonald et al. (1996) cited postflight changes in the phase-plane description of knee joint kinematics during gait as preliminary evidence for changes in joint impedance resulting from exposure to weightlessness.

The aim of the present study was to determine the effects of microgravity exposure on the astronauts' performance of two-footed jump landings. This study was intended to elucidate how exposure to an altered gravitational environment affects control of lower limb impedance and preprogrammed motor strategies for impact absorption. The joint kinematics of the lower extremity during the jump landings, as well as the kinematics of the whole-body mass center, were of particular interest. The results suggest that different subjects adopt one of two response modes upon return to 1 *g* following space flight, and that postflight performance differences may result largely from adaptive changes in open-loop lower limb impedance modulation. The altered jumping kinematics seen postflight may reflect decrements in limb proprioception, altered interpretation of otolith acceleration cues, and reduced requirements for maintenance of posture under microgravity conditions.

Materials and methods

Experiment design

The subject pool for this study consisted of nine NASA Space Shuttle astronauts. In order to protect the subjects' anonymity, they will henceforth be designated by letter codes (S-1, S-2,...S-9). Informed consent was obtained for all experiments, human use approval was granted for the study by the NASA Johnson Space Center Institutional Review Board for Human Research, and the experiments have therefore been performed in accordance with the ethical standards laid down in the 1964 Declaration of Helsinki. Subjects were permitted to withdraw from the study at any time and for any reason. The subjects ranged in age from 36 to 50 years. The astronauts were in good health and showed no signs of vestibular or postural control deficits. Of the nine subjects, eight were men and one was a woman. The first preflight testing (PRE1) took place 2–6 months before launch. Another preflight test (PRE2) occurred 9–15 days prior to launch, while the postflight tests (POST) were performed within 4 h of Shuttle landing. Mission lengths varied between 7 and 14 days. Preflight tests were performed in the Neuroscience Laboratory at the Johnson Space Center in Houston, Texas. Postflight testing took place at the landing site (either Edwards Air Force Base, Calif., or the Kennedy Space Center, Fla.).

At each data collection session, the jumping protocol consisted of six voluntary, two-footed downward hops from a 30-cm platform. Three jumps were performed while fixating continuously on a

Table 1 Number of significant differences in preflight and postflight variables (*COM* center of mass)

Measure	Subjects exhibiting significant change (*n*): Preflight: PRE1 vs PRE2	Subjects exhibiting significant change (*n*): PRE1&PRE2 vs POST	Ratio of no. changes (PRE1&PRE2 vs POST)/(PRE1 vs PRE2)
Peak hip angle	4	3	0.75
Peak knee angle	3	8	2.67
Peak ankle angle	5	6	1.20
Peak hip rate	2	7	3.50
Peak knee rate	2	6	3.00
Peak ankle rate	1	1	1.00
Peak COM deflection	2	4	2.00
Time from impact to peak COM deflection	0	4	∞
Peak COM upward recovery velocity	3	3	1.00

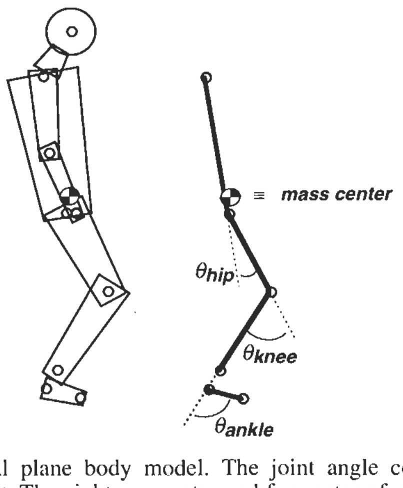

Fig. 1 Sagittal plane body model. The joint angle convention is shown at *right*. The eight segments used for center of mass calculation (feet, shanks, thighs, trunk, forearms, upper arms, neck, and head) are shown schematically on the *left*. Reflective marker positions are denoted by *o*

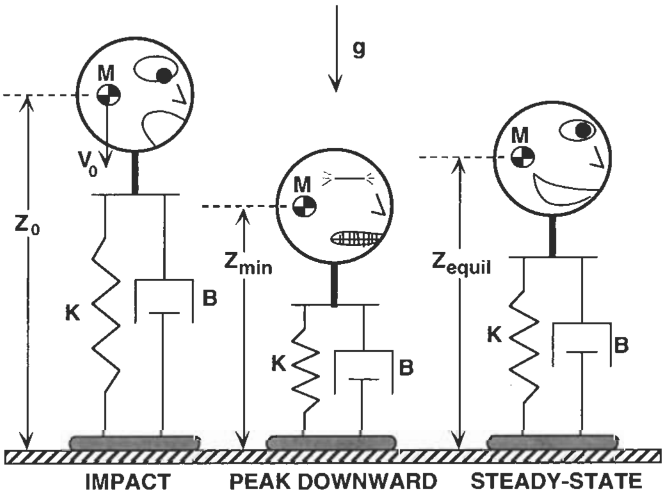

Fig. 2 One-degree-of-freedom, 2nd-order model for vertical (Z) center of mass (COM) motion following impact. Body mass (M), located at the COM, is supported by linear spring (K) and dashpot (B). The unloaded length of the spring is Z_0 (nominally the height of the COM at impact), minimum spring length is Z_{min}, and the spring length at the final equilibrium is Z_{equil}

ground target 1 m forward of the subject's initial toe position. The other three jumps were performed with the eyes closed; so subjects were instructed to look at the ground target then close their eyes and fixate on the imagined ground target position during the jump. Eyes open (EO) and eyes closed (EC) trials were alternated. Because of safety concerns related to subject instability postflight, the first jump was always performed with the eyes open. The subjects were instructed to land on both feet at the same time, although no specific instructions were given regarding the jump takeoff. A safety harness connected to an overhead frame prevented subjects from falling to the floor, but did not interfere with mobility during a normal jump.

Whole-body kinematics data were collected with a video-based motion-analysis system (Motion Analysis Corporation, Santa Rosa, Calif.). This system tracked the three-dimensional position of 14 passive reflective markers placed on the body. Markers were placed on the right side of the body at the toe, ankle, malleolus, knee, hip, shoulder, elbow, wrist, and ear. The remaining markers were located at the left heel and along the body centerline at the sacral bone, C7, occipital prominence, and head vertex. For some of the subjects, foot switches located in the shoes underneath the heel and great toe of both feet were used to record the times when the feet were in contact with the ground.

Data analysis

The motion analysis system provided the marker positions in three dimensions at a sampling rate of 60 Hz. The ankle, knee, and hip joint angles in the right leg were computed using the positions of the markers at the toe, ankle, knee, hip, and shoulder (see Fig. 1). These calculations assumed that the foot, shank, thigh, and trunk were rigid segments. For all three joints, larger positive joint angles represented greater joint flexion, while negative values denoted joint extension. In order to account for the possibility of variation in marker placement from session to session, mean resting joint angles during quiet standing were calculated for each data collection session. These mean resting angles were subtracted from the joint angle time series data for that session. Hence, the data shown here represent deviations from quiet standing posture, and positive joint angles indicate increased flexion from the rest position. Joint angular velocities were found by numerically differentiating the joint angle data using a four-point centered difference. Before differentiating, the angle data were smoothed by filtering forward and backward (to eliminate phase shift) using a 3rd-order Butterworth filter with a corner frequency of 15 Hz. Impact resulted in large and nearly instantaneous increases in the joint angular velocities. In order to avoid excessive smoothing of this feature, the data segments prior to and following impact were filtered and differentiated separately. Care was taken to minimize startup and ending filter transients by matching initial conditions.

The time of foot impact with the ground was extracted from the foot switch data for those subjects who were tested using the switches. For the other subjects, the impact time was calculated by determining when the downward velocity of the toe marker dropped to less than 10 mm/s. Comparisons of the two methods for finding impact time in the subjects with foot switch data yielded excellent agreement. For each jump, peak flexion angles and flexion rates after impact were computed for the ankle, knee, and hip joints as well as joint angles at the time of impact.

The position of the whole-body center of mass (COM) in the sagittal plane was estimated from the marker positions, using an eight-segment body model (feet, shanks, thighs, trunk, upper arms, forearms, neck, and head). Lateral symmetry was assumed, allowing combination of the left and right segments in the arms and legs. The approximate distribution of the body mass among the body segments was found using a regression model based on the subject's weight and height (McConville et al. 1980; Young et al. 1983). COM position was computed in an x-z coordinate system, where the x-value represented the fore-aft position and the z-direction corresponded to the gravitational vertical. Positive values for x and z corresponded to forward and upward, respectively. The velocity of the COM was found using the same numerical differentiation procedure described above for the joint angular velocities.

Initial analysis of the joint and COM kinematics indicated a nonuniform pattern of postflight responses across the subject pool. Therefore, preflight and postflight data sets were compared for each subject individually for peak joint flexion angles, peak joint flexion rates, and three COM-related measures: (1) maximum downward deflection, (2) time from impact to maximum downward deflection, and (3) peak upward recovery velocity. A two-way analysis of variance (ANOVA) was used to examine the effects of test session (PRE1, PRE2, POST) and vision (EO, EC). Test session effect was computed two ways: (1) PRE1 compared with PRE2, and (2) PRE1 and PRE2 together compared with POST. Tests yielding $P < 0.05$ were considered statistically significant.

Changes preflight to postflight in nine measures (three peak joint angles, three peak joint rates, and three COM quantities) were considered for classification of the subjects into groups based on postflight performance. For each quantity, the number of subjects showing a significant change between the two preflight sessions was compared with the number demonstrating a significant difference between preflight and postflight (Table 1).

Of the nine measures, five were selected for classification purposes, because they proved relatively insensitive to day-to-day variations. These measures (peak knee angle, peak hip and knee rates, peak COM deflection, and time to peak COM deflection) showed differences between pre- and postflight in at least twice as many subjects as they did between the two preflight sessions. The five variables were tested together for the effects of test session and vision, using a two-way multivariate ANOVA (MANOVA). Again, the contrast for test session effect was computed for preflight compared with postflight. Probabilities were based on Wilks' Lambda (likelihood ratio criterion) and Rao's corresponding approximate (sometimes exact) *F*-statistic. Subjects who did not exhibit significant differences between pre- and postflight for the multivariate measure were classified as "no change" (N-C).

The other subjects were classified as either "postflight compliant" (P-C) or "postflight stiff" (P-S) by scoring the five individual measures used in the MANOVA. For each measure, the subject received a "+1" for a significant change toward greater compliance postflight, a "−1" for a significant change toward lower compliance postflight, and a zero for no significant change. The results for the individual measures were summed to get an overall score ranging from −5 to +5. Subjects with positive scores were designated P-C, while negative scores were labeled P-S. All statistical computations were performed using SYSTAT (Wilkinson 1989).

Model of COM vertical motion

A simple mechanical body model was developed to investigate the vertical motion of the COM following impact with the ground. In this single degree-of-freedom model (Fig. 2), the vertical (z) motion was assumed to decouple from the horizontal motion, which was neglected. The entire body mass was concentrated at the COM, supported by a mass-less, constant-stiffness Hookean spring representing the legs. Similar models have been used by Alexander and Vernon (1975) and McMahon and Cheng (1990) to examine hopping and running. The upward restoring force exerted by the spring was proportional to the downward displacement of the COM from the uncompressed spring length Z_0 (nominally the height of the COM at the moment of impact). Energy dissipation, or damping, was modeled by a linear dashpot in parallel with the leg spring, which opposed the COM motion with a force proportional to COM velocity.

This model led to a 2nd-order linear differential equation that describes the COM motion:

$$M\ddot{z} + B\dot{z} + K(z - Z_0) = Mg \quad (1a)$$

$$\ddot{z} + \frac{B}{M}\dot{z} + \frac{K}{M}(z - Z_0) = g \quad (1b)$$

where z, $\dot{z}$, $\ddot{z}$ are COM vertical position, velocity, and acceleration, respectively; g is gravitational acceleration; M isbody mass; $B$is damping; and K is spring stiffness. The initial conditions needed to find the time solution of the equations are given by the vertical position and velocity of the COM at the moment of impact. In order to compare the pre- and postflight limb impedance properties for each subject, best-fit values for each jump were determined for the coefficients $\frac{K}{M}$ and $\frac{B}{M}$ (the stiffness and damping, respectively, normalized by subject body mass). The best-fit values were found using the MatLab System Identification Toolbox (The MathWorks, Natick, Mass.). Model fitting was accomplished by minimizing a quadratic prediction error criterion using an iterative Gauss-Newton algorithm (Ljung 1993). The best fit for the rest spring length Z_0 was determined concurrently, although this parameter was nominally set by the height of the COM at impact. Unfortunately, the sampling rate was too low to provide an adequate estimate of the Z_0 value: with COM velocities greater than 2 m/s at impact, an uncertainty of one sampling interval in the time of impact could result in errors in Z_0 exceeding 3 cm. Since peak deflection of the COM following impact typically ranged from 8 to 15 cm, this level of uncertainty required simultaneous estimation of the spring length using the MatLab identification routines.

Equation 1 can be rewritten in canonical 2nd-order form:

$$\ddot{z} + 2\zeta\omega_n\ddot{z} + \omega_n^2(z - Z_0) = g \quad (2)$$

where

$$\omega_n = \sqrt{\frac{K}{M}} = \text{natural frequency}$$

and

$$\zeta = \frac{B}{2\sqrt{KM}} = \text{damping ratio.}$$

The natural frequency is roughly equivalent to the bandwidth of the system and provides a measure of the speed of response, since higher natural frequencies correspond to faster transient responses. Clearly, increasing the stiffness K leads to a higher natural frequency. The damping ratio measures how oscillatory the transient response is, with lower damping ratios indicating more overshoot and oscillation or "ringing" in the system behavior. Increasing the stiffness K decreases the damping ratio, as does reducing the damping coefficient B.

Results

Joint kinematics

Phase-plane plots, where joint angular velocities (degrees per second) are plotted against the joint angles (degrees), yield the best format for comparing the joint kinematics of several jumps. Figure 3a shows phase portraits for subject S-1 comparing a time-synchronized mean of 12 preflight and six postflight jumps for the hip, knee, and ankle joints. The time of impact is marked by an open circle on each plot in Fig. 3, and the plots are traversed in the clockwise direction through the impact absorption and recovery to an upright posture. In general, after impact the peak flexion rate is reached rapidly; the peak flexion rate is the uppermost point on the phase portrait. Moving further along the phase diagram, the joint angular velocities drop to zero as the muscles act to decelerate the body's downward motion. When the joint flexion rate reaches zero, the joint is at its peak flexion angle, the rightmost point on the plot. After this point, the flexion rate becomes negative, indicating joint extension as the subject recovers to the upright resting posture. These plots depict means of the jumps for the preflight and postflight sessions, with the time scales for each data series synchronized at the time of foot impact with the ground.

The plots for subject S-1 clearly illustrate expanded postflight phase diagrams for each joint with respect to the preflight measurements. Postflight, this subject exhibits greater peak joint flexion angles than during the preflight jump landings, indicating that the subject reached a more crouched body position postflight while absorbing the impact from the jump. Furthermore, the peak joint angular velocities seen postflight are greater than the joint rates observed preflight. In contrast, the phase-plane diagrams for subject S-9 in Fig. 3b demonstrate the opposite

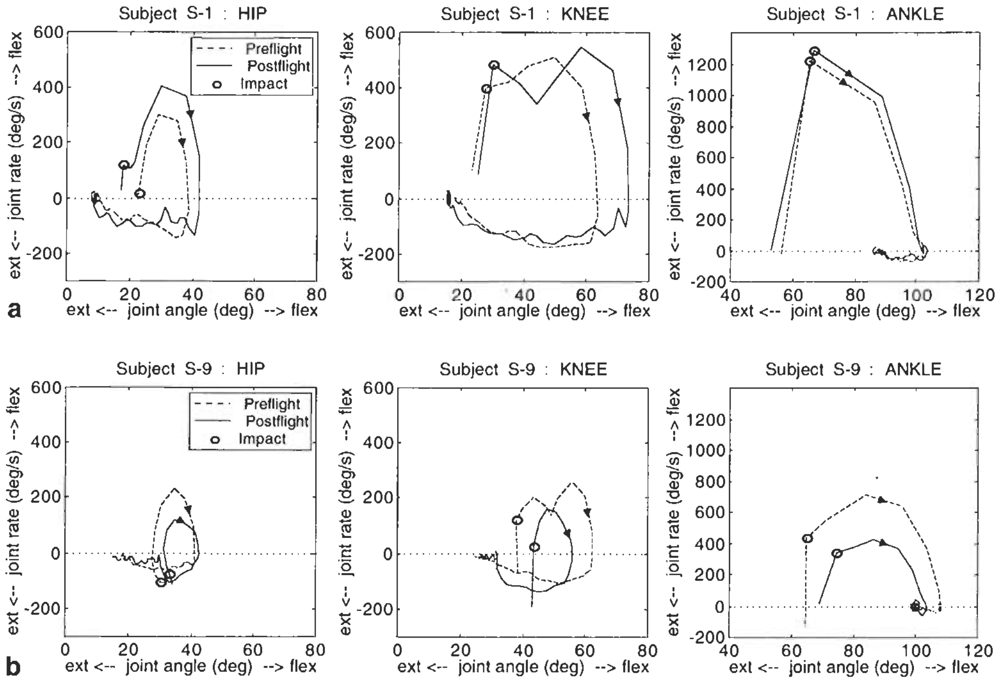

Fig. 3a, b Comparison of preflight (*dashed*) and postflight (*solid*) joint angle phase-plane portraits for hip, knee, and ankle. **a** For subject S-1, the postflight phase diagram is expanded with respect to the preflight diagram. **b** In contrast, subject S-9 demonstrates postflight contraction of the phase portrait in comparison with preflight results

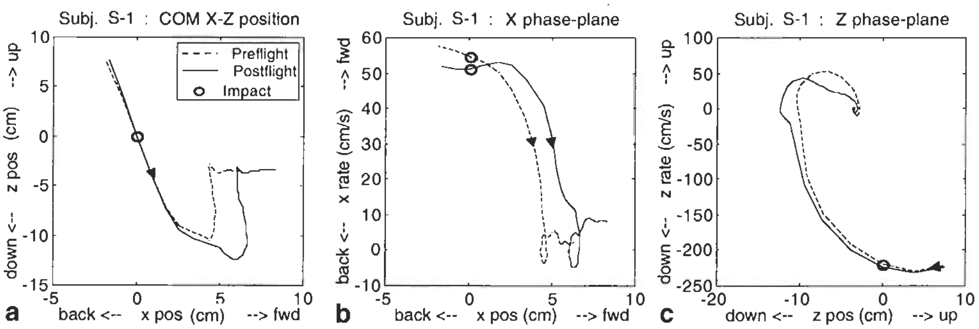

Fig. 4a–c Comparison of preflight (*dashed*) and postflight (*solid*) COM motion for postflight-compliant subject S-1. **a** The trajectory of the COM in the sagittal (*X-Z*) plane; peak deflection of the COM is greater postflight. **b** Phase-plane motion of the COM in the *X* (horizontal) direction is shown. **c** *Z* (vertical) motion, indicating greater downward deflection and slower upward recovery postflight

effect; the postflight portraits are consistently smaller than the plots of the preflight jumps. This postflight contraction of the phase diagrams denotes a decrease in peak joint flexion postflight, indicating that this subject retained a more upright posture while absorbing the impact. In addition, this subject shows smaller peak joint flexion rates in postflight testing than in the preflight jumps.

Center of mass kinematics

As with the joint angle data, the kinematics of the COM are plotted in a phase-plane format. Figure 4 shows the COM motion for subject S-1. Once again, the plots depict means of the 12 preflight and six postflight trials. Figure 4a shows the mean motions of the COM in the x-z (sagittal) plane. Figure 4b, c presents the phase-plane trajectories in the x (fore-aft) and z (vertical) directions traversed in the clockwise direction, respectively. The open circles in Fig. 4b, c denote the moment of impact coinciding with peak downward COM velocity. Deceleration of the COM downward motion takes place until the COM is at its lowest point and the z velocity is zero. Then the z velocity becomes positive as the COM recovers to the steady state value for standing posture. The peak upward velocity occurs at the uppermost point on the trajectory. The trajectory may spiral in around the equilibrium point if there is oscillation about the final steady state position.

Subject classification

The joint angle phase diagrams for these two astronauts suggest that the subjects who exhibit postflight changes in joint kinematics compared with preflight values may be divided into two distinct groups. Using the analogy of a spring of variable stiffness, the first group is denoted P-C. Just as a more compliant spring compresses more under a given load, this group generally exhibits greater joint flexion postflight than preflight, accompanied by increased postflight flexion rates. The second group is labeled P-S, indicating lower peak flexion and flexion rates for the jump landings following space flight.

Table 2 Subject classification based on kinematic measurements

Subject	S-1	S-2	S-3	S-4	S-5	S-6	S-7	S-8	S-9
Peak knee Flexion	+1	+1	+1	+1	+1			−1	−1
Peak knee Flexion rate	+1	+1	+1	+1	+1				−1
Peak hip Flexion rate	+1	+1	+1	+1	+1		+1		−1
Peak COM deflection	+1	+1	+1					−1	
Time to peak COM deflection	+1	+1	+1						−1
Overall score	+5	+5	+5	+3	+3	0	+1	−2	−4
P-value	0.005	0.003	0.002	0.003	0.277	0.275	0.051	0.002	4×10^{-6}
Classification	**P-C**	**P-C**	**P-C**	**P-C**	N-C	N-C	N-C	**P-S**	**P-S**

The COM kinematics provide complementary information for classification of subject performance following space flight. If the legs are considered to be roughly springlike in supporting the mass of the upper body, the maximum downward deflection of the COM following impact gives a measure of the stiffness of the lower limb "spring" (e.g., an *increase* in the downward deflection of the mass center indicates a *decrease* in the spring stiffness). The time from impact to the point of peak downward deflection also provides an indicator of the effective stiffness of the lower limbs. A decrease in the time between impact and maximum deflection implies an increase in the stiffness.

Table 2 contains the scoring of the five measures used to classify each subject. Positive entries indicate significant changes toward greater compliance postflight, corresponding to increases in peak joint angles or peak joint flexion rates, greater downward COM deflection, or longer times from impact to maximum COM vertical deflection. Negative entries represent significant differences in these quantities that indicate greater stiffness postflight. The statistical significance for the preflight/postflight MANOVA contrast of the five measures are shown for each subject. As previously mentioned, subjects with significant MANOVA results were denoted P-C or P-S, based on positive or negative overall scores, respectively, for the five classification measures; the remainder were designated.

Four subjects (S-1, S-2 , S-3 , S-4) were classified P-C. All four had significantly increased peak knee flexion combined with significantly greater peak knee and hip flexion rates postflight; for three of the four (all except S-4), COM downward deflection and the time from impact to peak COM downward deflection also increased postflight. Both of the subjects designated P-S (S-8 and S-9) exhibited significantly decreased peak knee flexion postflight. Subject S-9 also showed significant decreases in peak hip and knee flexion rates after space flight, as well as a decrease in the mean time from impact to peak COM downward deflection. Peak COM downward deflection was significantly reduced for subject S-8. The remaining three subjects (S-5, S-6, S-7) did not show a significant change between preflight and postflight based on the multivariate criterion.

Because the measures of peak joint angle, peak joint rate, and maximum COM vertical deflection are affected by the magnitude of the impact force as well as lower limb stiffness, the changes observed cannot be attributed to limb impedance changes unless the impact loading is the same pre- and postflight. For this reason, the COM vertical velocity at the moment of impact was compared for each subject's pre- and postflight jumps. Only two subjects (S-9 and S-2) showed significant differences between pre- and postflight impact velocities at the $P < 0.05$ level. For subject S-9, the mean postflight impact velocity was reduced by almost 20% compared with the preflight jumps. This change probably contributed to the decrease in knee flexion, joint rates, and COM displacement observed for this subject. Subject S-2 also exhibited a significant postflight decrease of about 5% in impact velocity. In spite of the postflight reduction in impact loading, subject S-2 exhibited consistent *increases* in peak joint flexion, flexion rate, and COM downward deflection. Thus, the impact velocity result actually adds support to the P-C classification for S-2. All other P-C and P-S subjects showed small, nonsignificant differences between pre- and postflight COM impact velocity.

In summary, the P-C subjects exhibit significant increases in postflight joint flexion and flexion rates; the P-S subjects show the opposite effect, although the trend is less apparent in subject S-8. Figure 5a compares the mean preflight and postflight values for maximum knee flexion, based on two preflight sessions of six jumps each and one postflight session of six jumps. Figure 5b and c contains pre- and postflight peak flexion rates for the knee and hip joints, respectively. Figure 6a and b shows the preflight and postflight values for the two COM-related measures: peak downward COM deflection and time from impact to peak deflection. With the exception of subject S-4, all of the P-C and P-S subjects demonstrate a significant change in one or both of the COM measures, supporting their classification.

Group means for pre- and postflight data were also calculated for the P-S subjects, the P-C subjects, and all subjects taken together, and are shown at the right in Figs 5 and 6. Taken as a group, the P-C subjects show significant increases in all five measures. Grouping the two P-S subjects reveals significant decreases in peak knee flexion and maximum COM downward deflection.

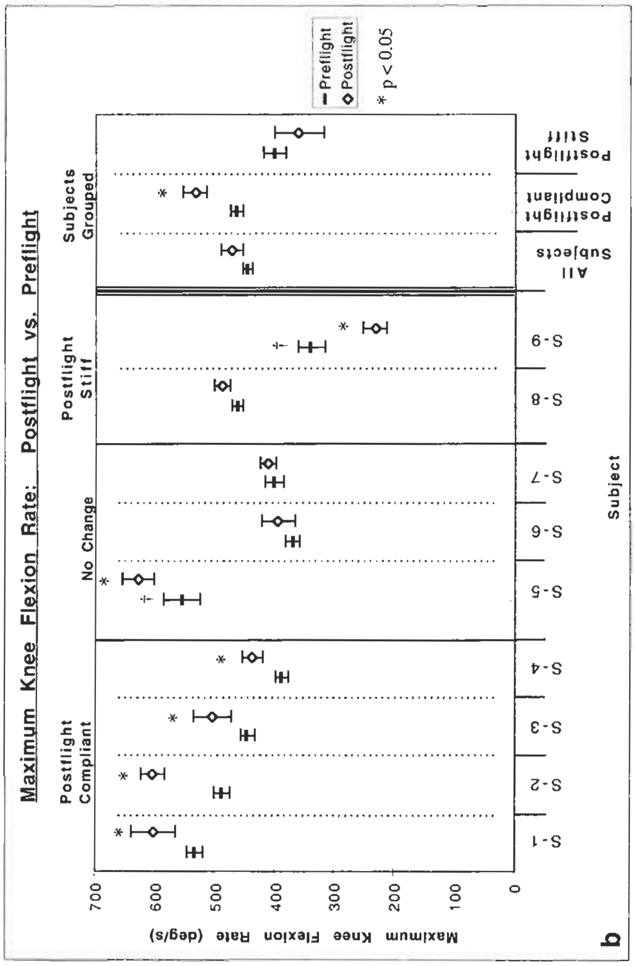

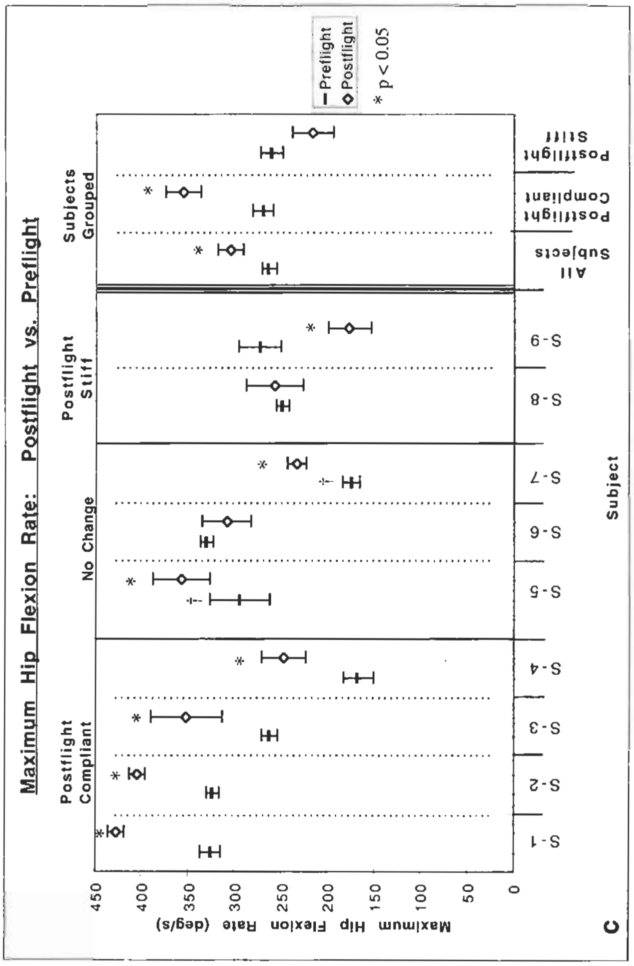

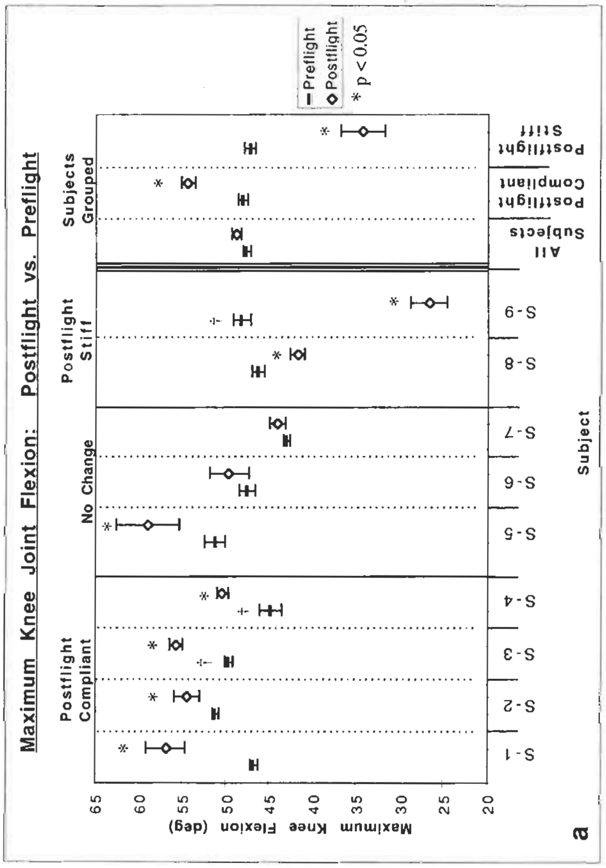

Fig. 5a–c Mean preflight and postflight maximum values for nine astronaut subjects. Levels of statistical significance are denoted by an *asterisk* ($P < 0.05$) and *error bars* indicate the SEM. A "dagger" indicates a significant test-day effect for the contrast between the two preflight sessions. **a** Joint flexion angles following impact from a 30-cm jump for the knee. **b** Peak joint flexion rate following impact for the knee. **c** Peak joint flexion rate following impact for the hip

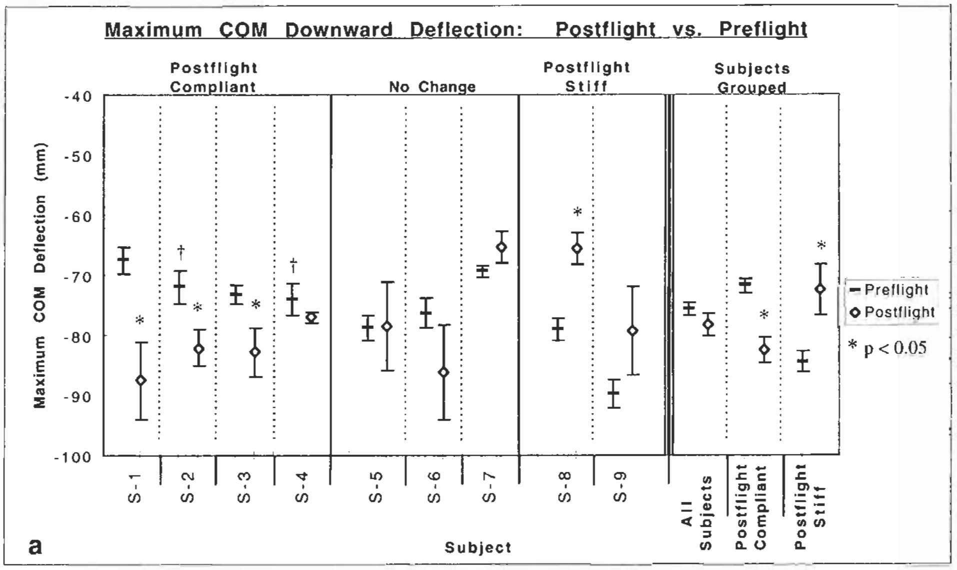

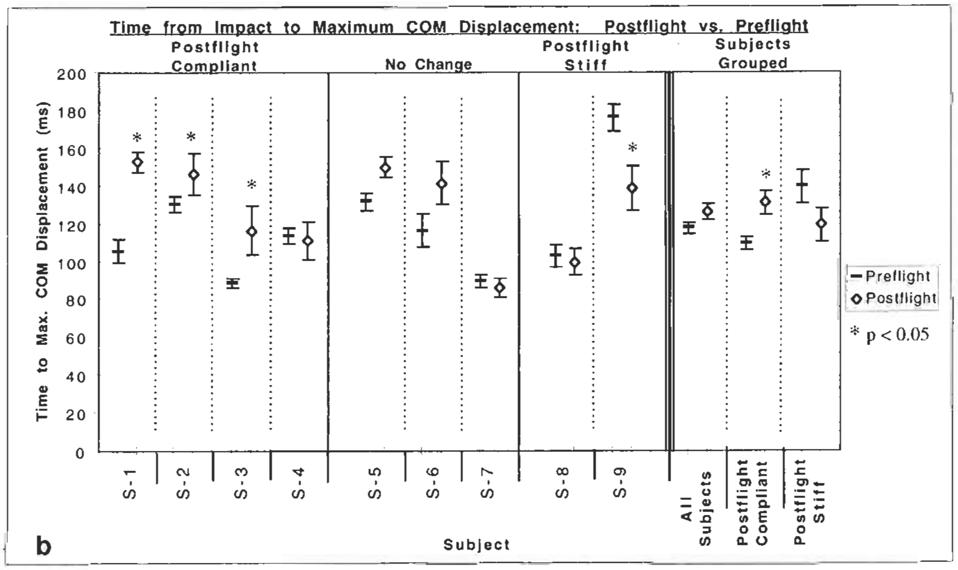

Fig. 6a, b COM displacement. Levels of statistical significance are denoted by an *asterisk* ($P < 0.05$) and *error bars* indicate the SEM. A "dagger" indicates a significant test-day effect for the contrast between the two preflight sessions. **a** Mean preflight and postflight maximum downward deflection of the COM following impact. **b** Time from impact to maximum COM downward displacement

Modeled COM vertical motion

Figure 7 shows predicted COM model responses using parameters estimated for representative pre- and postflight jumps for P-C subject S-1. Model fits for the 12 preflight (Fig. 7a, top) and six postflight (Fig. 7a, bottom) trials are staggered along the vertical axis. Figure 7b shows preflight (top) and postflight (bottom) mean COM vertical trajectories. Simulated model results using the pre- and postflight stiffness and damping means are included as well. The COM motion in the preflight jump exhibits a substantial overshoot above the final equilibrium posture, indicating a fairly low damping ratio. The postflight jump shows a much slower response with little overshoot. Thus, the postflight response is consistent with a decreased natural frequency and increased damping ratio in comparison to the preflight jump. P-S subjects, in contrast, demonstrate the opposite trend toward faster responses postflight with greater overshoot.

Table 3 summarizes the stiffness and damping coefficients that were estimated for each subject and show an excellent match with the subject classification based on kinematics. Note that these values have been normalized by the subject body mass and modeled stiffnesses are shown in Fig. 8. All four P-C subjects (S-1, S-2 , S-3, and S-4) and S-5 show large (23–55%), statistically significant decreases in postflight stiffness compared with preflight values. Stiffness increases for P-S subjects S-8 and S-9 were not significant. The surprising lack of a significant postflight stiffness increase for subject S-9 (considering the consistent P-S changes in the joint and COM kinematics) may be due to this subject's postflight decrease in impact velocity. The change in impact loading is explicitly accounted for in the COM motion model.

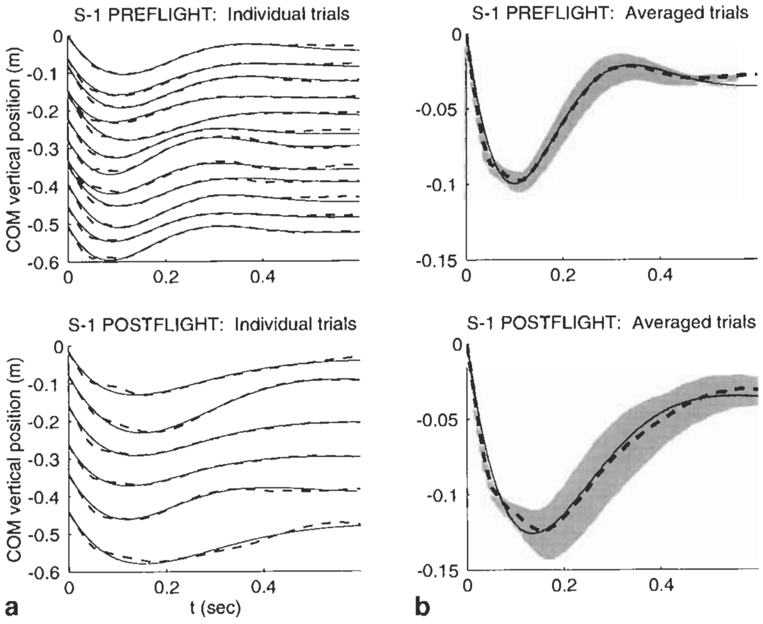

Fig. 7a, b Modeled COM vertical motion using stiffness and damping estimated for representative pre- and postflight jumps for P-C subject S-1. *Dashed lines* are experimental data and *solid lines* represent model fits. **a** Twelve individual preflight trials (*top*) and six postflight trials (*bottom*). **b** Corresponding means for trials shown in **a**. The origin represents time synchronization of jump landings at impact. The *shaded region* denotes ± 1 SD

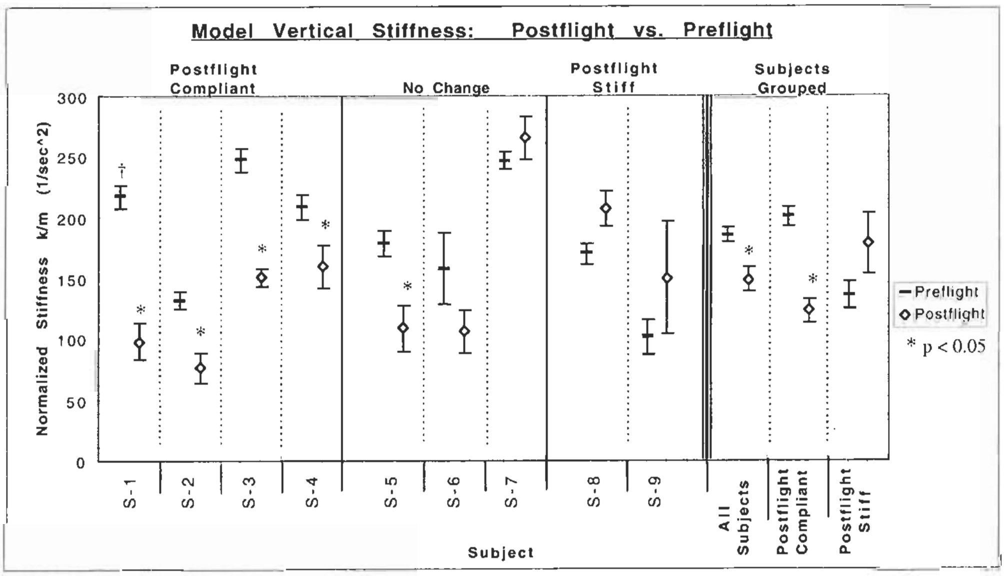

Fig. 8 Mean preflight and postflight model vertical stiffnesses. Levels of statistical significance are denoted by an *asterisk* ($P < 0.05$) and *error bars* indicate the SEM. A "dagger" indicates a significant test-day effect for the contrast between the two preflight sessions

Table 3 Stiffness and damping in 2nd order model

Subject	Stiffness (k/m) ($1/s^2$)				Damping (b/m) ($1/s$)			
	Pre-flight	Post-flight	Change (%)	P-value	Pre-flight	Post-flight	Change (%)	P-value
S-1	217.2	98.3	–54.7%	0.0001	14.2	12.8	–9.7%	0.1490
S-2	132.0	76.6	–42.0%	0.0007	14.0	14.0	+0.1%	0.7150
S-3	247.2	150.7	–39.1%	0.0001	16.2	12.5	–22.9%	0.0030
S-4	208.2	159.9	–23.2%	0.0240	13.7	12.5	–8.6%	0.0740
S-5	178.6	108.9	–39.0%	0.0100	12.3	13.4	+9.5%	0.2630
S-6	158.3	106.3	–32.8%	0.1990	14.6	14.8	+1.8%	0.6590
S-7	247.1	265.4	+ 7.4%	0.3230	15.2	16.2	+6.5%	0.3030
S-8	170.5	207.8	+21.9%	0.0510	14.4	13.6	–5.9%	0.2280
S-9	101.4	150.4	+48.3%	0.1720	12.8	13.7	+7.1%	0.4620

Table 4 Second-order response parameters

Subject	Natural frequency, ω_n				Damping ratio, ζ			
	Pre-flight	Post-flight	Change (%)	*P*-value	Pre-flight	Post-flight	Change (%)	*P*-value
S-1	14.7	9.8	−33.3%	0.0001	0.49	0.66	+36.5%	0.0004
S-2	11.4	8.6	−24.6%	0.0003	0.61	0.83	+35.4%	0.0010
S-3	15.7	12.3	−21.8%	0.0001	0.52	0.51	−2.5%	0.7600
S-4	14.4	12.6	−12.7%	0.0200	0.48	0.50	+5.6%	0.2850
S-5	13.3	10.3	−22.5%	0.0090	0.47	0.67	+43.0%	0.0100
S-6	14.3	10.1	−18.0%	0.1870	0.61	0.74	+20.7%	0.1020
S-7	15.7	16.2	+3.4%	0.3260	0.49	0.50	+3.0%	0.5920
S-8	13.0	14.4	+10.5%	0.0540	0.56	0.48	−14.7%	0.0090
S-9	9.8	11.7	+20.0%	0.1500	0.68	0.61	−10.4%	0.2600

In contrast with the changes in stiffness, examination of the damping coefficients reveals few differences between pre- and postflight performance, with only subject S-3 exhibiting a significant change (decrease). Furthermore, there is no apparent pattern of increases or decreases in the level of damping that corresponds to either subject classification or the changes in stiffness.

From the definitions of w_n and z in Eq. 2, a decrease in stiffness for a constant damping level should result in a lower natural frequency and a higher damping ratio. The calculated values for w_n and z are shown in Table 4. As anticipated, the four P-C subjects all exhibit significant decreases of 13%-33% in the natural frequency as well as S-5, and hence reduced bandwidth postflight. Four of these subjects have increased damping ratios postflight as well, although significant changes are seen only for subjects S-1, S-2, and S-5. The P-S subjects demonstrate the opposite trend: increased natural frequency postflight, combined with decreases in the damping ratio (significant only for S-8 damping ratio).

Discussion

Pre- and postflight comparisons of the joint kinematics during jump landings indicate that the astronaut subjects may be separated into two different classes based on examination of the phase-plane descriptions, namely P-C and P-S. The P-C group exhibits expanded phase-plane portraits postflight in comparison with preflight baseline data, and the P-S group shows the contrary. The lower leg musculature may be thought of as contributing a resistance to joint displacements, or stiffness (modeled as a torsional spring-like element), as well as a resistance to joint angular velocity, or damping (represented by a viscous damper or dashpot). These stiffness and damping elements represent the displacement and velocity-dependent components of the joint impedance, respectively.

Using this description, the P-C group exhibits postflight increases in the majority of both peak joint flexion angles and rates indicating a *reduction* in stiffness about the joints following microgravity exposure. In these subjects, increases in joint flexion provide quantitative support for the reports of Watt et al.'s (1986) astronaut subjects that their legs were bending more during drop landings postflight. These changes are also consistent with reductions in joint torques and a reduction in the bandwidth of the postural control system as a whole. In contrast, two of the subjects demonstrated an opposite, P-S response after returning from space flight. Their postflight contraction in the phase-plane plots indicates increases in limb stiffness and bandwidth of the postural controller.

A number of possible explanations exist for the observed changes in joint impedance during these jump landings, including loss of strength in the antigravity musculature, altered sensory feedback (muscle stretch reflexes, vestibular, or visual), and changes in open-loop modulation of limb stiffness. Since the stiffness and damping that can be exerted about a joint are directly related to the forces in the muscles acting about the joint, significant strength decreases in the antigravity muscles of the legs could well account for the expanded phase-plane portraits observed in the P-C group of astronauts. However, the P-S subjects exhibit postflight increases in stiffness indicating *increased* joint torques; thus, the results from these subjects undermine the hypothesis that loss of muscle strength alone can account for the observations in this study.

Sensory feedback

Sensory feedback pathways also contribute to the stiffness and damping of the closed-loop postural control system. Feedback quantities that could play a role in the jump landings include postural muscle stretch (modulated through spinal reflexes), vestibular sensing of head orientation and angular velocity, and visual inputs. The stretch reflexes effectively increase the stiffness about the joints by recruiting additional muscle fibers to counteract perturbations to the muscle lengths; the stretch reflexes in concert with Golgi tendon organ force feedback probably serve to modulate the tension-length behavior (impedance) of the muscles. Gurfinkel (1994) reported decreases in the strength of the stretch reflex in tibialis anterior following space flight; Kozlovskaya et al. (1981) found amplitude reductions in Achilles tendon stretch reflexes after long-duration flight. Such decreases could have the effect of reducing the stiffness about the leg joints, and hence the stiffness of the leg "spring" supporting the body mass. However, Melvill Jones and Watt (1971a) demonstrated that the monosynaptic stretch response (occurring approximately 40 ms after forcible dorsiflexion of the foot) did not contribute to gastrocnemius muscle tension. Rather, the development of force was found to correspond to a sustained electromyographic (EMG) burst with a latency of 120 ms following dorsiflexion stimuli, which they termed the "functional stretch reflex." Since the peak joint angle deflections in the jump landing occur only 100 ms after impact, stretch reflex activity is unlikely to play a major role in the impact absorption phase.

Studies by Allum and Pfaltz (1985) and Greenwood and Hopkins (1976) found vestibulospinal reflex latencies for postural muscles of 80 ms. Visual influences were found to be delayed 80 ms and 100 ms, respectively by Allum and Pfaltz (1985) and Nashner and Berthoz (1978). These latencies comprise most of the interval from impact to peak joint deflections, indicating that sensory feedback information from these sources following impact cannot be expected to contribute significantly to the impact absorption phase of jump landings. However, vestibular and visual inputs during the takeoff and flight phases of the jump may contribute to the motor activity during impact absorption. Interestingly, in the current study the eyes were closed in half of the jumps without a measurable effect on performance, indicating that vision's effect during the jump landings was minimal. This qualitative finding is intriguing in light of evidence for increased dependence on visual cues following space flight for posture control and perception of body orientation and self-motion (Young et al. 1986). However, McKinley and Smith (1983) describe jump-down behavior in normal and labyrinthectomized cats with and without vision and conclude that normal cats that jumped from a known height did not rely on visual input to program prelanding EMG responses, but, when jump height was uncertain and visual input was absent, they speculate that vestibular input became more important. In our study, the astronaut subjects had full knowledge of the jump height after the first jump, which was always conducted with the eyes open. Furthermore, even in the EC jumps, the subjects had visual information about the jump height even though they closed their eyes immediately prior to jumping. Therefore, the apparent ability to program prelanding responses without vision may account for the lack of difference in jumps with and without vision.

Limb stiffness

The limitations on the sensory feedback pathways indicate that the stiffness properties of the lower limbs may be largely predetermined before impact. The stiffness about the joints is determined by the level of muscle activation, and the overall impedance of the leg to COM motion is also affected by the configuration of the limbs at impact (in general, less joint flexion results in greater vertical stiffness due to the reduction of the moment arm about the joint centers). McKinley and Pedotti (1992) found that the knee extensor muscles (rectus femoris and vastus lateralis) were activated slightly before impact while the ankle plantarflexors (gastrocnemius and soleus) were continuously active from midflight during jumps. Furthermore, the legs reached their largest extension before impact, and were already slightly flexed again by the time of impact. Other investigators (Dyhre-Poulsen and Laursen 1984; Thompson and McKinley 1988) have determined that the timing of the preparatory muscle activation and limb configuration is keyed to the expected time of impact. For downward stepping and repetitive hopping, Melvill Jones and Watt (1971a) found that muscular activity commenced from 80 to 140 ms prior to ground contact and concluded that the deceleration associated with landing was due to a preprogrammed neuromuscular activity pattern rather than stretch reflex action.

Melvill Jones and Watt (1971b) demonstrated activation of both gastrocnemius and tibialis anterior approximately 75 ms following an unexpected fall; this reflex activity is most likely due to vestibular system otolith inputs. Such activation of antagonist muscles would contribute to stiffening of the limbs prior to impact. Furthermore, Watt et al. (1986) showed that the amplitude of this response is markedly decreased during space flight. However, Watt's tests on landing day showed that the response had returned to normal almost immediately postflight, so changes in the otolith-spinal reflex may not account for the changes observed in the jumps described here. Reschke et al. (1986) used the H-reflex to examine the effect of drops on the sensitivity of the lumbosacral motoneuron pool, which is presumably set by descending postural control signals. A large potentiation of the H-reflex (recorded in the soleus muscle) was found beginning approximately 40 ms following an unexpected drop. Furthermore, the investigators found that, on the 7th day of space flight, the potentiation of the H-reflex during drops vanished. Immediately following space flight, two of four subjects demonstrated a significant increase in potentiation during the drop compared with preflight testing. While an increase or decrease in the sensitivity of the motoneuron pool might correspond to respective increases or decreases in the leg stiffness via a gain change in the spinal reflex pathway, the link to preprogrammed muscular activity is not clear.

In addition to the muscular commands linked to the flight and impact phases of the jump, the underlying tonic activation in the leg musculature may contribute to the impedance in the lower limbs during jump landing. Clément et al. (1984) found an increase in tonic ankle flexor activity combined with a decrease in tonic extensor activity during space flight, which if carried over postflight could lead to a reduction in the stiffness about the ankle joint against gravitational loads. It is well established that suppression of vestibular function results in depression of the gamma-static innervation to the leg extensors, causing reduction in extensor tone (Molina-Negro et al. 1980). However, because relative enhancement of the knee flexor was not observed, Clément's group viewed the changes at the ankle as a "subject-initiated postural strategy" rather than a functional deafferentation of the otoliths due to microgravity. Regardless of the origin, significant changes in leg muscle tone could well contribute to altered leg stiffness postflight.

Modeled stiffness

The hypothesis that the joint impedance characteristics transform into lumped leg stiffness and damping parameters governing the vertical COM motion following impact provides the basis for the mechanical model postulated in this paper. These parameters are assumed to remain constant through the impact absorption and recovery to upright stance. McMahon and Cheng (1990) summarized evidence indicating that the legs behave much like a linear spring of near-constant stiffness over a wide range of forces and running speeds. Based on those arguments and the generally close fits to experimental data obtained for the jumps in the present study, the simplifying assumptions of constant stiffness and damping appear reasonable. The constant leg stiffness value that best described human running in McMahon and Cheng's 1990 model was approximately 150 N/m per kilogram, falling well within the range of stiffness computed for the jump landings here.

Comparison of the pre- and postflight fits for this model indicates that variations in the model parameters can adequately predict the alterations in COM motion seen in astronaut jump landings following space flight. More specifically, changes in the leg stiffness alone appear to govern the differences in transient response observed upon return to earth. The postflight decreases and increases in the vertical leg stiffness found for these subjects correspond to the classifications of P-C and P-S made previously on the basis of kinematics alone.

In the model, decreases in leg stiffness lead to decreases in bandwidth, with slower and less oscillatory time responses. In contrast, increased stiffness results in faster, higher bandwidth performance with greater overshoots. These decreases and increases in leg stiffness postflight match the changes found in the transient performance for the P-C and P-S subjects, respectively. Interestingly, the model fits did not show changes in the leg damping to play a significant role in the postflight differences. This result is counterintuitive, since an increase in antagonist muscle activation to raise the limb stiffness might be expected to cause a corresponding increase in the mechanical damping properties of the muscles as well.

Furthermore, changes in damping in accordance with increases or decreases in stiffness would help to prevent large deviations in the damping ratio (see Eq. 2), which is often desirable from a control system standpoint. Regardless, the evidence presented here indicates that the damping properties of the limbs can be modulated independently of the stiffness, or simply that the damping characteristics are largely constant in the face of large changes in leg stiffness.

The final equilibrium positions predicted by the model lie somewhat below the actual final COM rest values, implying that the stiffness for these model fits is less than the values that would have been calculated from the final equilibria alone. In many cases, it was not possible to find parameter values that gave good predictions for both the transient portion of the response and the steady state equilibrium. Because this study focused on impedance modulation during the impact absorption phase of the jump, the parameter estimation procedure was designed to find best fits for the transient portion of the response, often resulting in differences between the predicted and actual equilibrium positions. Interestingly, the pattern seen in Fig. 7 was consistent across the subject pool: on average, predicted equilibria lay below the actual values. This result was attributed to a transition in control mode and limb posture from the impact absorption phase to the maintenance of upright posture near equilibrium. In equilibrium posture control, the flexed joints and greater compliance used in impact absorption give way to the more upright resting stance, where the alignment of the leg joints results in high vertical stiffness.

The changes in the model parameters corresponding to altered joint and mass center kinematics observed in the astronauts postflight were probably due to changes in the preprogrammed muscle activity prior to impact, which sets the limb impedance in an open-loop fashion by controlling the muscle tension-length properties and the limb configuration. The changes observed in this study in the impact absorption phase support the notion that space flight contributed to altered neuromuscular activity during the flight phase of the jump, even though EMG records were not available. The presumed alterations in muscle activation patterns following space flight could reflect changes in the relative recruitment of antagonist muscles, or differences in the timing of activation (e.g., failure to activate antigravity muscles early enough during the flight phase to stiffen the limbs for impact).

Conclusions

From an operational standpoint, the results of this study are important for understanding how microgravity exposure might impair astronauts' abilities to perform tasks such as an emergency egress from the Space Shuttle, or even locomotion on another planet following an extended duration-space flight. The postflight changes in the kinematics of astronaut jump landings reported here have been attributed to changes in the control of the lower limb impedance due to exposure to the microgravity conditions of space flight. The decreased stiffness of the posture control system observed in the P-C group of subjects may reflect inflight adaptation to the reduced requirements for posture control in the absence of gravitational forces. On the ground, the nature of the body's compound inverted pendulum structure requires the maintenance of a certain minimum stiffness for stability in an upright position. In space, the body need not be stabilized against gravity, and the control bandwidth and stiffness may therefore be reduced without compromising postural stability. Inflight, an overall reduction in postural stiffness may be observed as reduction in extensor tone and decreases in stretch reflex gain and may be related to the loss of drop-induced H-reflex potentiation. Compliant postflight behavior may result from a residual decrement in the stiffness of the postural control system following return to earth. In contrast, stiff postflight behavior may indicate overcompensation for reduced inflight stiffness upon return to earth, similar to the "rebound" effect observed by Reschke et al. (1986) for the H-reflex. Thus, stiff responses postflight may be related to the observation by Young et al. (1986) that some subjects were able to maintain balance only within a narrow "cone of stability" postflight, especially with the eyes closed. By using a stiffening strategy postflight, the subject minimizes deviations from equilibrium to avoid approaching the boundaries of the cone of stability. Such stiffening in turn requires a commensurate increase in postural control bandwidth.

In summary, this study provides evidence for modulation of lower limb impedance by astronauts in response to exposure to the microgravity of space flight. The results reported here, interpreted in light of other studies, indicate that this impedance modulation may result from a combination of altered tonic muscular activity and changes in the preprogrammed neuromuscular activity observed prior to and during impact absorption. Simulations using a simple mechanical model of the COM vertical motion indicate that changes in the lumped leg stiffness cause the differences in postflight jumping performance seen in the joint and COM kinematics. The reduced requirements for maintenance of posture under microgravity conditions probably contribute to the changes seen postflight, in concert with decrements in limb proprioception and altered interpretation of otolith acceleration cues.

Acknowledgements We thank Brian Peters and Shannon Smith for their help with the experiments and data acquisition, the astronauts who participated in this study, and Dr. Vernon McDonald for his helpful insights. This work supported by NASA grant NGT-51228, NASA contract NAS1-18690, and NASA NAGW 4336.

References

Alexander RM, Vernon A (1975) Mechanics of hopping by kangaroos (Macropodidae). J Zool 177:265–303

Allum JHJ, Pfaltz CR (1985) Visual and vestibular contributions to pitch sway stabilization in the ankle muscles of normals and patients with bilateral peripheral vestibular deficits. Exp Brain Res 58:82–94

Bloomberg JJ, Peters BT, Huebner WP, Smith SL, Reschke MF (1997) Locomotor head-trunk coordination strategies following space flight. J Vestib Res 7:161–177

Chekirda IF, Bogdashevskiy AV, Yeremin AV, Kolosov IA (1971) Coordination structure of walking of Soyuz-9 crew members before and after flight. Kosm Biol Med 5:48–52

Clément G, Gurfinkel VS, Lestienne F, Lipshits MI, Popov KE (1984) Adaptation of postural control to weightlessness. Exp Brain Res 57:61–72

Dyhre-Poulsen P, Laursen AM (1984) Programmed electromyographic activity and negative incremental muscle stiffness in monkeys jumping down. J Physiol (Lond) 350:121–136

Greenwood R, Hopkins A (1976) Muscle responses during sudden falls in man. J Physiol (Lond) 254:507–518

Gurfinkel V (1994) The mechanisms of postural regulation in man. Sov Sci Rev F Physiol Gen Biol Rev 7:59–89

Homick JL, Reschke MF (1977) Postural equilibrium following exposure to weightless space flight. Acta Otolaryngol 83:455–464

Kenyon RV, Young LR (1986) M.I.T./Canadian vestibular experiments on the Spacelab-1 mission. 5. Postural responses following exposure to weightlessness. Exp Brain Res 64:335–346

Kozlovskaya IB, Kriendich YV, Oganov VS, Koserenko OP (1981) athophysiology of motor functions in prolonged manned space flights. Acta Astronaut 8:1059–1072

Layne CS, McDonald PV, Pruett CJ, Jones G, Bloomberg JJ (1995) Preparatory postural control after space flight. Soc Neurosci Abstr 21:138

Ljung L (1993) System identification toolbox user's guide. MathWorks, Natick, Mass

Martin TP, Edgerton VR, Grindeland RE (1988) Influence of spaceflight on rat skeletal muscle. J Appl Physiol 65:2318–2325

McConville J, Churchill T, Kaleps I, Clauser C, Cuzzi J (1980) Anthropometric relationships of body and body segment moments of inertia. Anthropology Research Project, Aerospace Medical Division, AFSC Technical Report AFAMRL-TR-80-119, Wright-Patterson Air Force Base, Ohio

McDonald PV, Basdogan C, Bloomberg JJ, Layne CS (1996) Lower limb kinematics during treadmill walking after space flight: Implications for gaze stabilization. Exp Brain Res 112:325

McKinley P, Pedotti A (1992) Motor strategies in landing from a jump: the role of skill in task execution. Exp Brain Res 90:427–440

McKinley P, Smith J (1983) Visual and vestibular contributions to prelanding EMG during jump-downs in cats. Exp Brain Res 52:439–448

McMahon TA, Cheng GC (1990) The mechanics of running: how does stiffness couple with speed? J Biomech [Suppl 1] 23:65–78

Melvill Jones G, Watt DGD (1971a) Muscular control of landing from unexpected falls in man. J Physiol (Lond) 219:729–737

Melvill Jones G, Watt DGD (1971b) Observations on the control of stepping and hopping movements in man. J Physiol (Lond) 219:709–727

Molina-Negro P, Bertrand RA, Martin E, Gioani Y (1980) The role of the vestibular system in relation to muscle tone and postural reflexes in man. Acta Otolaryngol 89:524–533

Nashner LM, Berthoz A (1978) Visual contribution to rapid motor responses during postural control. Brain Res 150:403–407

Paloski WH, Black FO, Reschke MF, Calkins DS, Shupert C (1993) Vestibular ataxia following shuttle flights: Effects of transient microgravity on otolith-mediated sensorimotor control of posture. Am J Otol 14:9–17

Parker DE, Reschke MF, Arrott AP, Homick JL, Lichtenberg BK (1985) Otolith tilt-translation reinterpretation following prolonged weightlessness: Implications for preflight training. Aviat Space Environ Med 56:601–606

Reschke MF, Anderson DJ, Homick JL (1986) Vestibulo-spinal response modification as determined with the H-reflex during the Spacelab-1 flight. Exp Brain Res 64:367–379

Thompson HW, McKinley PA (1988) Effect of visual perturbations in programming landing from a jump in humans. Soc Neurosci Abstr 14:66

Watt DGD, Money KE, Bondar RL, Thirsk RB, Garneau M, Scully-Power P (1985) Canadian medical experiments on Shuttle flight 41-G. Can Aeronaut Space J 31:215–226

Watt DGD, Money KE, Tomi LM (1986) M.I.T./Canadian vestibular experiments on the Spacelab-1 mission. 3. Effects of prolonged weightlessness on a human otolith-spinal reflex. Exp Brain Res 64:308–315

Wilkinson L (1989) SYSTAT: the system for statistics. SYSTAT, Evanston, Ill

Young J, Chandler R, Snow C (1983) Anthropometric and mass distribution characteristics of the adult female. Civil Aeromedical Institute, Federal Aviation Administration, Report FAA-AM-83-16, Oklahoma City, OK

Young L, Oman C, Watt D, Money K, Lichtenberg B, Kenyon R, Arrott A (1986) M.I.T./Canadian vestibular experiments on the Spacelab-1 mission. 1. Sensory adaptation to weightlessness and readaptation to one-*g*: an overview. Exp Brain Res 64:291–298